Resolving Lambertian surface orientation from fluctuating radiance

Nicholas C. Makris[a] and Ioannis Bertsatos
Department of Mechanical Engineering, Massachusetts Institute of Technology, Cambridge, Massachusetts 02139

(Received 25 January 2010; revised 28 February 2011; accepted 6 March 2011)

A maximum likelihood method for estimating remote surface orientation from multi-static acoustic, optical, radar, or laser images is presented. It is assumed that the images are corrupted by signal-dependent noise, known as speckle, arising from complex Gaussian field fluctuations, and that the surface properties are effectively Lambertian. Surface orientation estimates for a single sample are shown to have biases and errors that vary dramatically depending on illumination direction. This is due to the signal-dependent nature of speckle noise and the nonlinear relationship between surface orientation, illumination direction, and fluctuating radiance. The minimum number of independent samples necessary for maximum likelihood estimates to become asymptotically unbiased and to attain the lower bound on resolution of classical estimation theory are derived, as are practical design thresholds. © *2011 Acoustical Society of America*. [DOI: 10.1121/1.3570949]

PACS number(s): 43.30.Pc, 43.30.Re [WLS] Pages: 1222–1231

I. INTRODUCTION

Acoustic, optical, radar, and laser images of remote surfaces are typically corrupted by signal-dependent noise known as speckle. This noise arises when wavelength scale roughness on the surface causes a random interference pattern in the field scattered from it by an active system. Relative motion between source, surface and receiver, or source incoherence causes the received field to fluctuate over time with circular complex Gaussian random (CCGR) statistics.[1–5] Underlying these fluctuations, however, is the expected radiance of the surface, from which its orientation may be inferred. In many cases of practical importance, Lambert's law is appropriate for such inference because variations in the projected area of a surface patch, as a function of source and receiver orientation, often cause the predominant variations in its radiance.

The aim of this paper is to provide a method for estimating the orientation and albedo of a remote Lambertian surface from measurements of fluctuating radiance, which are corrupted by speckle noise arising from CCGR fluctuations. The ability to accurately resolve remote surface orientation from measurements of fluctuating radiance is not only of great importance to ocean acoustics,[6,7] but also to optics,[8,9] medical ultrasound,[10] planetary terrain surveillance,[11,12] and machine vision.[13] Active underwater acoustic imaging systems such as acoustic cameras[14–16] typically measure echoes returning from the marine environment with a two-dimensional (2D) or three-dimensional (3D) array. Images are then formed through beamforming and focusing either by digital signal processing or by the use of physical acoustic lenses.[14] Acoustic imaging systems of this kind are typically implemented to reconstruct and interpret underwater scenes that often contain a variety of objects with distinct shapes and sizes. Acoustic cameras, for example, have recently been used to map the microbathymetry of a seafloor strewn with ancient pottery at an underwater archaeological site,[17] inspect tubular structural members in offshore oil platforms,[18] detect submerged mines, and determine the shape of individual swimming fish.[19] Most Navy surface ships and submarines employ 2D or 3D active imaging arrays that form pencil beams for underwater surveillance.[6] Acoustic imaging systems are also widely used in medical ultrasound, where, for example, 3D echocardiography[20] employs real-time volumetric imaging[21] with a pyramidal-beam formed by a volume array of transducers.

All measurements made from sonar imaging systems are inherently corrupted by speckle noise. Due to the signal-dependent nature of speckle noise, and the often nonlinear relationship between surface orientation, illumination direction, and radiance,[22] surface orientation estimates based on a single sample typically have large biases and mean-square errors (MSEs). A large number of samples may then be necessary to yield surface orientation estimates with tolerable biases and MSEs depending on the relative orientation of the surface with respect to the imaging system's source and receiver. Given the probability distribution of surface radiance and the physical model relating it to surface orientation and albedo, maximum likelihood estimates (MLEs) are derived and their biases and variances are expanded in terms of the likelihood function.[23–26] The likelihood function governs the physical and statistical behavior of surface orientation estimates, so that the expansions presented here are guaranteed to converge in inverse orders of sample size or signal-to-noise ratio (SNR). Analytical expressions are then derived for the sample sizes or SNRs necessary to obtain estimates that are in the asymptotic regime where biases are negligible and MSEs attain minimum variance. The biases and errors are found to vary significantly with illumination direction and measurement diversity. The minimum error in estimating the angle of incidence with respect to a Lambertian

[a]Author to whom correspondence should be addressed. Electronic mail: makris@mit.edu

surface, for example, is shown to be at best proportional to the *cotangent* of this angle, so that surface orientation varies from irresolvable at normal incidence to perfectly resolvable at shallowest grazing. A preliminary investigation of surface orientation estimation from fluctuating intensity presented by Makris at the SACLANT 1997 conference[27] determined sample size conditions by a Taylor series approach that is not guaranteed to converge in inverse orders of sample size as the approach here does since it did not involve the expansion of the likelihood function. The special case of deterministic data, which corresponds to infinite SNR, has been treated by Horn.[13]

In Sec. II, we present the necessary radiometry background and describe how measurements of surface radiance are typically obtained, and in Sec. III, we give the probability density for such radiometric measurements. In Sec. IV, we review estimation theory and the maximum likelihood method, and determine necessary conditions on sample size or SNR to obtain estimates of the desired accuracy. Finally, in Sec. V we present illustrative examples of estimating surface orientation and albedo.

II. RADIOMETRY

The flux $d\Phi$, received in a acoustic, optical, radar, or laser beam of solid angle $d\beta$, is related to the area of the resolved surface patch dA_β (Fig. 1), the local surface radiance L_β, and the solid angle subtended by the receiver aperture $d\Omega$, by the linear equation

$$d\Phi = dA_\beta L_\beta d\Omega. \tag{1}$$

The solid angle subtended by the receiver aperture from the surface patch dA_β is $d\Omega = \cos\psi_r\, dA/r^2$, where dA is the area of the aperture, $\cos\psi_r$ is the foreshortening of the surface patch with respect to the receiver, ψ_r is the scattering angle, and r is the range to the aperture. The intensity of the received beam is then

$$I_\beta = \frac{d\Phi}{dA} = dA_\beta L_\beta \frac{\cos\psi_r}{r^2}. \tag{2}$$

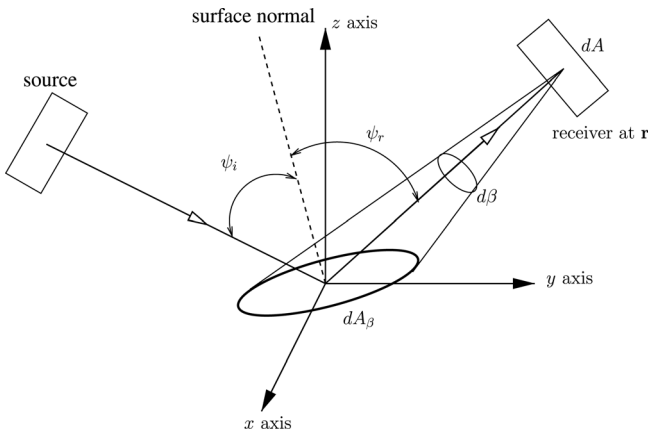

FIG. 1. Resolved surface patch.

Assuming that the receiver is of sufficiently high resolution that it resolves an elemental surface patch dA_β, that is locally planar and small enough so that

$$d\beta = dA_\beta \frac{\cos\psi_r}{r^2}, \tag{3}$$

surface radiance can be directly measured by the receiver as

$$\frac{dI_\beta}{d\beta} = L_\beta. \tag{4}$$

For a Lambertian surface,

$$L_\beta = \rho E \cos\psi_i, \tag{5}$$

so that the radiance measured in an acoustic, optical, radar, or laser image of the scene L_β, is independent of the viewing direction ψ_r. It follows a linear relationship with the foreshortening $\cos\psi_i$ of the surface patch, the surface irradiance E, and the surface bidirectional reflectance distribution function ρ which is $1/\pi$ for a perfectly reflecting Lambertian surface. Here ψ_i is the angle of incident insonification and E is defined as incident flux per unit area on the surface of albedo $\pi\rho$.

III. THE LIKELIHOOD FUNCTION AND MEASUREMENT STATISTICS

Let the stochastic measurement vector $\mathbf{R}$ of length M contain the independent statistics R_k whose expected values $\sigma_k(\mathbf{a}) = \langle R_k \rangle$ are linearly related to measured surface radiance, where the vector $\mathbf{a}$ contains the surface orientation parameters a_r to be estimated from the measurements $\mathbf{R}$ for $r = 1, 2, 3, \ldots, Q$. More succinctly, let $\boldsymbol{\sigma}(\mathbf{a}) = \langle \mathbf{R} \rangle$.

Assuming the R_k are corrupted by CCGR field fluctuations, the conditional probability distribution for the measurements $\mathbf{R}$ given parameter vector $\mathbf{a}$ is the product of gamma distribution[5,28]

$$P_{\mathbf{R}}(\mathbf{R};\mathbf{a}) = \prod_{k=1}^{M} \frac{\left(\frac{\mu_k}{\sigma_k(\mathbf{a})}\right)^{\mu_k} (R_k)^{\mu_k - 1} \exp\left(-\mu_k \frac{R_k}{\sigma_k(\mathbf{a})}\right)}{\Gamma(\mu_k)}. \tag{6}$$

The quantity μ_k is the number of coherence cells in the measurement average used to obtain R_k,[5,28] the variance of which is given by σ_k^2/μ_k. It is important to note that μ_k is then also equal to the squared-mean-to-variance ratio, or SNR, defined as $\langle R_k \rangle^2 / (\langle R_k^2 \rangle - \langle R_k \rangle^2)$. For example, μ_k equals the time-bandwidth product of the received field if each R_k is obtained from a continuous but finite-time average. Additionally, μ_k can be interpreted as the number of stationary speckles averaged over a finite spatial aperture in the image plane or the number of stationary multi-look images averaged for a particular scene.[28]

IV. CLASSICAL ESTIMATION THEORY AND A HIGHER ORDER ASYMPTOTIC APPROACH TO INFERENCE

The maximum likelihood estimator $\hat{\mathbf{a}}$, for the parameter set $\mathbf{a}$, maximizes the log-likelihood function $l(\mathbf{R};\ \mathbf{a}) = \ln(P_{\mathbf{R}}$

$(\mathbf{R};\ \mathbf{a})$) with respect to $\mathbf{a}$. The Cramer–Rao lower bound (CRLB) $\mathbf{i}^{-1}$ is the minimum MSE attainable by any unbiased estimate, regardless of the method of estimation. The CRLB is the inverse of the Fisher information matrix, also known as the expected information, the elements of which are given by $i_{bc} = \langle l_b l_c \rangle$, where $l_r = \partial l(\mathbf{R};\mathbf{a})/\partial a_r$ and a_r is the rth component of $\mathbf{a}$.

For sufficiently large sample size, μ_k, the MLE is asymptotically unbiased and follows the Gaussian distribution

$$P_{\hat{\mathbf{a}}}(\hat{\mathbf{a}};\mathbf{a}) = \sqrt{\frac{|\mathbf{i}|}{(2\pi)^M}} \exp\left(-\frac{1}{2}(\hat{\mathbf{a}}-\mathbf{a})^T \mathbf{i}(\hat{\mathbf{a}}-\mathbf{a})\right), \tag{7}$$

with variance $\mathbf{i}^{-1}$ equal to the CRLB,[29,30] where[5,28]

$$i_{bc} = \sum_{k=1}^{M} \left(\mu_k \frac{\partial \ln \sigma_k(\mathbf{a})}{\partial a_b} \frac{\partial \ln \sigma_k(\mathbf{a})}{\partial a_c}\right), \tag{8}$$

and

$$i^{bc} \equiv [\mathbf{i}^{-1}]_{bc} = \sum_{k=1}^{M} \left(\frac{(\sigma_k(\mathbf{a}))^2}{\mu_k} \frac{\partial a_b}{\partial \sigma_k(\mathbf{a})} \frac{\partial a_c}{\partial \sigma_k(\mathbf{a})}\right) \tag{9}$$

given the probability distribution for $\mathbf{R}$ described in Eq. (6). In the deterministic limit $\mu_k \to \infty$, where the R_k are obtained from exhaustive sample averages, $P_{\hat{\mathbf{a}}}(\hat{\mathbf{a}};\mathbf{a})$ becomes the delta function $\delta(\hat{\mathbf{a}}-\mathbf{a})$.

Assume n independent identically distributed samples of the total measurement vector $\mathbf{R}$ of length M. Let $\boldsymbol{\mu}^T = [\mu_1, \mu_2, \ldots, \mu_M]$ be the vector of sample size μ_k of measurement R_k for $k = 1, 2, \ldots, M$. The moments of $\hat{a}_r$ for $r = 1, 2, 3, \ldots, Q$ can be expressed as series of inverse powers of the sample size n, as in Eqs. (3)–(5) of Ref. 26, provided that the required derivatives of the likelihood function exist.[23] The MLE bias of $\hat{a}_r$ is then expressed as

$$\text{bias}(\hat{a}_r,\ \boldsymbol{\mu},\ n) = b_1(\hat{a}_r;\ \mathbf{a}, \boldsymbol{\mu},\ n) + b_2(\hat{a}_r;\ \mathbf{a}, \boldsymbol{\mu},\ n) + \text{higher order terms}, \tag{10}$$

where $b_j(\hat{a}_r;\mathbf{a},\ \boldsymbol{\mu},\ n) = b_j(\hat{a}_r;\ \mathbf{a}, \boldsymbol{\mu},\ 1)\ /n^j$ is the jth order bias, so that

$$\text{bias}(\hat{a}_r,\ \boldsymbol{\mu},\ n) = \frac{b_1(\hat{a}_r;\mathbf{a},\ \boldsymbol{\mu},\ 1)}{n} + \frac{b_2(\hat{a}_r;\mathbf{a},\ \boldsymbol{\mu},\ 1)}{n^2} + O\left(\frac{1}{n^3}\right), \tag{11}$$

where $O(n^{-3})$ represents integer powers n^{-3} and higher. Similarly, the MLE variance of $\hat{a}_r$ can be expressed as

$$\text{var}(\hat{a}_r,\ \boldsymbol{\mu},\ n) = \frac{\text{var}_1(\hat{a}_r;\mathbf{a},\ \boldsymbol{\mu},\ 1)}{n} + \frac{\text{var}_2(\hat{a}_r;\mathbf{a},\ \boldsymbol{\mu},\ 1)}{n^2} + O\left(\frac{1}{n^3}\right), \tag{12}$$

where the first-order variance, $\text{var}_1(\hat{a}_r;\mathbf{a},\ \boldsymbol{\mu},\ 1)/n$, the CRLB, is the asymptotic variance for large n.

General expressions for the first-order bias $b_1(\hat{a}_r;\mathbf{a},\ \boldsymbol{\mu},\ 1)$, and second-order variance $\text{var}_2(\hat{a}_r;\mathbf{a},\ \boldsymbol{\mu},\ 1)$ of an MLE appear in Eqs. (3)–(5) of Ref. 26. For the statistical model of Eq. (6), these expressions and Eq. (9) lead to

$$b_1(\hat{a}_r;\mathbf{a},\ \boldsymbol{\mu},\ 1) = -\sum_{k=1}^{M} \frac{1}{2}\frac{\sigma_k^2}{\mu_k}\frac{\partial^2 a_r}{\partial \sigma_k^2}, \tag{13}$$

$$\text{var}_1(\hat{a}_r;\mathbf{a},\ \boldsymbol{\mu},\ 1) = \sum_{k=1}^{M} \frac{\sigma_k^2}{\mu_k}\left(\frac{\partial a_r}{\partial \sigma_k}\right)^2, \tag{14}$$

$$\text{var}_2(\hat{a}_r;\mathbf{a},\ \boldsymbol{\mu},\ 1) = -\sum_{k=1}^{M} \frac{1}{\mu_k^2}\left[2\sigma_k^3 \frac{\partial a_r}{\partial \sigma_k}\frac{\partial^2 a_r}{\partial \sigma_k^2} + \sigma_k^4 \frac{\partial a_r}{\partial \sigma_k}\frac{\partial^3 a_r}{\partial \sigma_k^3} + \frac{1}{2}\sigma_k^4\left(\frac{\partial^2 a_r}{\partial \sigma_k^2}\right)^2\right] \tag{15}$$

Assuming for simplicity that $\mu_k = \mu$ for all k, the MLE bias and variance can then also be expressed as asymptotic series in inverse powers of μ (see Appendix)

$$\text{bias}(\hat{a}_r,\ \boldsymbol{\mu},\ 1) = \frac{b_1(\hat{a}_r;\mathbf{a},\ \mathbf{e},\ 1)}{\mu} + \frac{b_2(\hat{a}_r;\mathbf{a},\ \mathbf{e},\ 1)}{\mu^2} + O\left(\frac{1}{\mu^3}\right), \tag{16}$$

$$\text{var}(\hat{a}_r,\ \boldsymbol{\mu},\ 1) = \frac{\text{var}_1(\hat{a}_r;\mathbf{a},\ \mathbf{e},\ 1)}{\mu} + \frac{\text{var}_2(\hat{a}_r;\mathbf{a},\ \mathbf{e},\ 1)}{\mu^2} + O\left(\frac{1}{\mu^3}\right), \tag{17}$$

where the components of the vector $\mathbf{e}$ are $e_k = 1$ for $k = 1, 2, \ldots, M$. To simplify notation, let $\text{var}_j(\hat{a}_r;\mathbf{a},\ \mathbf{e},\ 1) \equiv \text{var}_j(\hat{a}_r;\mathbf{a})$ and $b_j(\hat{a}_r;\mathbf{a},\ \mathbf{e},\ 1) \equiv b_j(\hat{a}_r;\mathbf{a})$.

The value of μ necessary for $\hat{a}_r$ to become *asymptotically* unbiased is found by conservatively requiring the first-order bias to be an order of magnitude smaller than the true value of the parameter,

$$\mu = 10\left|\frac{b_1(\hat{a}_r;\mathbf{a})}{a_r}\right| = 10\left|\frac{\sum_{k=1}^{M}\sigma_k^2\frac{\partial^2 a_r}{\partial \sigma_k^2}}{2a_r}\right|. \tag{18}$$

Similarly, the value of μ necessary for the MLE variance to *asymptotically* attain the CRLB is found by requiring the second-order variance to be an order of magnitude smaller than the first-order variance, so that

$$\mu = 10\frac{|\text{var}_2(\hat{a}_r;\mathbf{a})|}{\text{var}_1(\hat{a}_r;\mathbf{a})} = 10\frac{\left|\sum_{k=1}^{M} 2\sigma_k^3\frac{\partial a_r}{\partial \sigma_k}\frac{\partial^2 a_r}{\partial \sigma_k^2} + \sigma_k^4\frac{\partial a_r}{\partial \sigma_k}\frac{\partial^3 a_r}{\partial \sigma_k^3} + \frac{1}{2}\sigma_k^4\left(\frac{\partial^2 a_r}{\partial \sigma_k^2}\right)^2\right|}{\sum_{k=1}^{M}\sigma_k^2\left(\frac{\partial a_r}{\partial \sigma_k}\right)^2}. \tag{19}$$

Only for values of μ satisfying these conditions, it is possible for the variance to be in the asymptotic regime where it is unbiased and continuously attains the CRLB.[26,31,32]

V. INFERRING LAMBERTIAN SURFACE ORIENTATION

For measurement k, a collimated source with known unit incident direction $\mathbf{s_k}$ irradiates a planar Lambertian surface with unknown unit normal vector $\mathbf{n}$. For each measurement, the receiver measures Lambertian surface radiance from any hemispherical position within view of the surface. For convenience, a Cartesian coordinate system (x, y, z) is adopted, with the origin in the center of the resolved surface patch, as shown in Fig. 1. Because surface incident irradiance E_k is presumed known, given knowledge of source power, directionality, and transmission characteristics to the surface, it can be deterministically scaled out of the measured surface radiance leaving $\sigma_{L_k}=\langle L_k\rangle/E_k$. When signal-independent additive CCGR noise of intensity $\sigma_{N_k}d\beta_k E_k$ is also measured with the radiant field from the surface, the expected measurement vector $\mathbf{R}$ becomes $\boldsymbol{\sigma}(\mathbf{a})=\boldsymbol{\sigma}_L(\mathbf{a})+\boldsymbol{\sigma}_N$.

Lambert's law for the expected radiometric component of the data is then

$$\langle \mathbf{R}\rangle_L = \boldsymbol{\sigma}_L(\mathbf{a}) = [\sigma_1(\mathbf{a}),\ldots,\ \sigma_M(\mathbf{a})]^T = \mathbf{S}\mathbf{x}, \tag{20}$$

where the matrix S is defined by

$$\mathbf{S}^T = [\mathbf{s}_1,\ \mathbf{s}_2,\ \mathbf{s}_3,\ldots,\mathbf{s}_M], \tag{21}$$

the vector $\mathbf{x}$ equals $\rho\mathbf{n}$.

The general problem is to determine both the Lambertian surface normal vector $\mathbf{n}$ and the albedo $\pi\rho$ from the fluctuating measurements $\mathbf{R}$. The surface normal is typically expressed in terms of the surface gradient components

$$\mathbf{n}^T = [-p_n,\ -q_n,\ 1]/(1+p_n^2+q_n^2)^{1/2}, \tag{22}$$

where

$$p_n = \frac{\partial z}{\partial x},\quad q_n = \frac{\partial z}{\partial y}, \tag{23}$$

or in terms of spherical coordinates

$$\mathbf{n}^T = [\cos\phi_n \sin\theta_n,\ \sin\phi_n \sin\theta_n,\ \cos\theta_n]. \tag{24}$$

A. MLEs of surface orientation and albedo

The 3D parameter vector $\mathbf{x}$ is to be estimated from the potentially over-determined M-dimensional measurement vector $\mathbf{R}$. From Eqs. (8) and (20), the MSE bound on any unbiased estimate $\tilde{\mathbf{x}}$ is

$$\langle(\tilde{\mathbf{x}}-\mathbf{x})(\tilde{\mathbf{x}}-\mathbf{x})^T\rangle \geq \mathbf{i}_{\mathbf{x}}^{-1} = [\mathbf{S}^T\mathbf{i}_{\boldsymbol{\sigma}}\mathbf{S}]^{-1}, \tag{25}$$

where $[\mathbf{i}_{\boldsymbol{\sigma}}]_{ij}=\delta_{ij}\mu_{ij}/\sigma_i^2$ is infinite when all incident vectors $\mathbf{s_k}$ are tangent to $\mathbf{n}$ in the absence of signal-independent noise.

To derive the MLE of the vector $\mathbf{x}=\rho\mathbf{n}$, the probability distribution for $\mathbf{R}$ in Eq. (6) is rewritten as

$$P_{\mathbf{R}}(\mathbf{R};\mathbf{x}) = \prod_{k=1}^{M} \frac{\frac{\mu_k}{\sigma_k(\mathbf{x})}\mu_k(R_k)^{\mu_k-1}\exp\left(-\mu_k\frac{R_k}{\sigma_k(\mathbf{x})}\right)}{\Gamma(\mu_k)}. \tag{26}$$

The MLE $\hat{x}_r$ maximizes the log-likelihood function $\ln(P_{\mathbf{R}}(\mathbf{R};\mathbf{x}))$ with respect to x_r, so that it satisfies

$$\frac{\partial\ln(P_{\boldsymbol{R}}(\boldsymbol{R};\mathbf{x}))}{\partial x_r} = \sum_{k=1}^{M}\frac{\mu_k}{\sigma_k}\left[\frac{R_k}{\sigma_k}-1\right]\frac{\partial\sigma_k}{\partial x_r}\bigg|_{x_r=\hat{x}_r} = 0 \tag{27}$$

where $\frac{\partial\sigma_k}{\partial x_r}$ is the (k, r) element of $\mathbf{S}$. Considering all the elements of $\mathbf{x}$, Eq. (27) can be rewritten in vector form as

$$\sum_{k=1}^{M}(\mathbf{S}_k)^T\frac{\mu_k}{\sigma_k}\bigg|_{\mathbf{x}=\hat{\mathbf{x}}} = \sum_{k=1}^{M}(\mathbf{S}_k)^T\frac{\mu_k R_k}{\sigma_k^2}\bigg|_{\mathbf{x}=\hat{\mathbf{x}}}, \tag{28}$$

or

$$[\mathbf{S}^T\mathbf{i}_{\boldsymbol{\sigma}}\boldsymbol{\sigma}]\big|_{\mathbf{x}=\hat{\mathbf{x}}} = [\mathbf{S}^T\mathbf{i}_{\boldsymbol{\sigma}}\mathbf{R}]\big|_{\mathbf{x}=\hat{\mathbf{x}}} \tag{29}$$

where $\mathbf{S}_k$ is the kth row of $\mathbf{S}$. The MLE, given linearity between x and σ is then given by

$$\hat{\mathbf{x}} = [\mathbf{S}^T\mathbf{i}_{\boldsymbol{\sigma}}\mathbf{S}]^{-1}\,\mathbf{S}^T\mathbf{i}_{\boldsymbol{\sigma}}(\mathbf{R}-\boldsymbol{\sigma}_N), \tag{30}$$

is unbiased and attains the error bound $\mathbf{i}_{\mathbf{x}}^{-1}$ of Eq. (25).

Given this information, the MLEs for albedo $\pi\hat{\rho}=\pi|\hat{\mathbf{x}}|$, surface normal $\mathbf{n}=\hat{\mathbf{x}}/\hat{\rho}$, cone and polar angles $\hat{\theta}_n=\cos^{-1}\hat{n}_3$, $\hat{\phi}_n=\tan^{-1}(\hat{n}_2/\hat{n}_1)$, and surface gradient components $\hat{p}_n=-(\hat{n}_1/\hat{n}_3)$, $\hat{q}_n=-(\hat{n}_2/\hat{n}_3)$, however, are not generally unbiased and do not generally have minimum variance except for sufficiently large sample sizes.

Taking the case where $\mathbf{R}$ is a 3D vector and $\boldsymbol{\sigma}_N$ is negligible, for example, the joint distribution for $\hat{\mathbf{x}}$ is[27]

$$p_{\tilde{\mathbf{x}}}(\hat{\mathbf{x}}|\mathbf{x}) = |\mathbf{s}_1\cdot\mathbf{s}_2\times\mathbf{s}_3|\,P_{\boldsymbol{R}}(\mathbf{S}\hat{\mathbf{x}}|\boldsymbol{\sigma}), \tag{31}$$

which leads to the respective joint distributions

$$p_{\text{grad}}(\hat{p}_n,\hat{q}_n,\hat{\rho}|p_n,q_n,\rho) = \frac{P_{\hat{\mathbf{x}}}(-\hat{\rho}\hat{p}_n(1+\hat{p}_n^2+\hat{q}_n^2)^{-1/2},\ -\hat{\rho}\hat{q}_n(1+\hat{p}_n^2+\hat{q}_n^2)^{-1/2},\ \hat{\rho}(1+\hat{p}_n^2+\hat{q}_n^2)^{-1/2}|\mathbf{x})}{\left|\hat{\rho}^2(1+\hat{p}_n^2+\hat{q}_n^2)^{-3/2}\right|}, \tag{32}$$

and

$$p_{\text{polar}}(\hat{\theta}_n, \hat{\phi}_n, \hat{\rho}|\theta_n, \phi_n, \rho) = \frac{P_{\hat{\mathbf{x}}}(\hat{\rho}\cos\hat{\phi}_n \sin\hat{\theta}_n,\ \hat{\rho}\sin\hat{\phi}_n \sin\hat{\theta}_n,\ \hat{\rho}\cos\hat{\theta}_n|\mathbf{x})}{\left|\hat{\rho}^2 \sin^2\hat{\theta}_n\right|}, \quad (33)$$

for the gradient and polar coordinate MLEs.

Returning to the general case when $\mathbf{R}$ is an M-dimensional vector, the asymptotic maximum likelihood distributions for surface orientation and albedo follow Eq. (7) when Eqs. (18) and (19) are satisfied.

B. The angle of incidence

Suppose that the angle of incidence ψ is to be estimated from a single measurement R, with mean $\sigma = \rho\ \cos\psi$ and variance σ^2/μ, given that the albedo $\pi\rho$ is known. From Eq. (8), the resulting MSE bound is the inverse of the (scalar) Fisher information

$$\langle(\tilde{\psi} - \psi)^2\rangle \geq i^{-1} = \frac{(\cos\tilde{\psi} + \sigma_N)^2}{\mu \sin^2\psi}, \quad (34)$$

for any unbiased estimate, $\tilde{\psi}$ which becomes

$$\langle(\tilde{\psi} - \psi)^2\rangle \geq i^{-1} = \frac{\cot^2\psi}{\mu}, \quad (35)$$

when the signal-independent noise is negligible. These expressions show resolution of the incident angle to be highest when the Lambertian surface is illuminated at shallow grazing and lowest when the surface is illuminated near normal incidence. This can be motivated physically by noting that for shallow-grazing angle illumination Lambert's law has a first-order dependence that is proportional to the incident angle. Conversely, for illumination near normal incidence Lambert's law is independent of the incident angle to first order. It is also significant that when the root mean-square error (RMSE) bound is finite, it can be reduced in proportion to the square-root of the sample size μ averaged to obtain the radiometric statistic R, as shown in detail in Sec. IV.

The MLE for the angle of incidence is

$$\tilde{\psi} = \cos^{-1}\left(\frac{R - \sigma_N}{\rho}\right). \quad (36)$$

Many of the potential benefits and difficulties associated with maximum likelihood estimation can be illustrated by examining the statistical properties of $\hat{\psi}$

For the remainder of this section, let σ_N be negligible, as may be expected in practical imaging systems expect at shallow grazing where ψ is very near $\pi/2$. First of all, because R is a gamma variate and can take on any positive definite value, the estimate $\hat{\psi}$ is real for $0 \leq R/\rho \leq 1$ and imaginary for $R/\rho > 1$. The probability that $\hat{\psi}$ is real is found to be $\gamma(\mu, \mu/\cos\psi)/\Gamma(\mu)$ by appropriately integrating $P_R(R|\psi)$. But this leaves finite probability $\Gamma(\mu,\mu/\cos\psi)/\Gamma(\mu)$ that $\hat{\psi}$ is imaginary. More specifically, let the statistic $\hat{\psi} = \hat{\psi}_r + \hat{\psi}_i$, where $\hat{\psi}_r$, $\hat{\psi}_i$ are the real and imaginary parts of $\hat{\psi}$ respectively. Then the statistic $\hat{\psi}$ is distributed according to

$$P_{\hat{\psi}}(\hat{\psi};\psi) = \rho \sin\hat{\psi} P_R(\rho\cos\hat{\psi};\psi) \text{ over } 0 \leq \hat{\psi} \leq \pi/2, \quad (37)$$

for $\hat{\psi}$ real, and

$$P_{\hat{\psi}}(\hat{\psi};\psi) = \rho \sinh\hat{\psi} P_R(\rho\cosh\hat{\psi};\psi) \text{ over } 0 \leq \hat{\psi} \leq \infty, \quad (38)$$

for $\hat{\psi}$ imaginary. The probability $\Gamma(\mu, \mu/\cos\psi)/\Gamma(\mu)$ that $\hat{\psi}$ is imaginary decreases as the angle of incidence ψ and sample size μ increase, as does the bias of $\hat{\psi}$.

Apparently, CCGR fluctuations in the radiant field can lead to unphysical MLEs of the incident angle ψ. This can be remedied by reconditioning the MLE, given ancillary information[33] that $\hat{\psi}$ is real, so that

$$P_{\hat{\psi},\text{Re}}(\hat{\psi};\psi) \equiv P_{\hat{\psi}}(\hat{\psi}|\hat{\psi} = \Re\{\hat{\psi}\};\psi) = \rho \sin\hat{\psi} P_R(\rho\cos\hat{\psi};\psi)\frac{\Gamma(\mu)}{\gamma(\mu, \mu/\cos\psi)}, \quad (39)$$

for $0 \leq \hat{\psi} \leq \pi/2$. Similarly, the probability that $\hat{\psi}$ is imaginary is defined as

$$P_{\hat{\psi},\text{Im}}(\hat{\psi};\psi) \equiv P_{\hat{\psi}}(\hat{\psi}|\hat{\psi} = \Im\{\hat{\psi}\};\psi) = \rho \sinh\hat{\psi} P_R(\rho\cosh\hat{\psi};\psi)\frac{\Gamma(\mu)}{\gamma(\mu, \mu/\cos\psi)}, \quad (40)$$

For sufficiently large sample size μ, the relationship between MLE $\hat{\psi}$ and data $\mathbf{R}$ approaches linearity, so that $\hat{\psi}$ obeys the Gaussian distribution

$$P_{\hat{\psi},\text{G}}(\hat{\psi};\psi) = \left(\frac{\mu}{2\pi\cot^2\psi}\right)^{1/2} \exp\left(-\frac{1}{2}\mu\frac{(\hat{\psi} - \psi)^2}{\cot^2\psi}\right), \quad (41)$$

with bias vanishing and variance equaling the inverse Fisher information, $\cot^2\psi/\mu$.

Figure 2 shows the probability densities of Eq. (39) (dashed-dotted line), Eq. (40) (dashed line), and Eq. (41) (solid line) for $\psi = 30°$. As the sample size μ increases, the correlation between $P_{\hat{\psi},\text{G}}$ and $P_{\hat{\psi},\text{Re}}$ approaches one, while $P_{\hat{\psi},\text{Im}}$ goes to zero. For the value of ψ used in these plots, a sample size of approximately 320 is necessary for the correlation between $P_{\hat{\psi},\text{G}}$ and $P_{\hat{\psi},\text{Re}}$ to become larger than 0.99. As the true value ψ increases, the necessary sample size to achieve a good correlation is found to decrease, as discussed earlier.

Following Sec. IV, $\hat{\psi}$ is effectively unbiased when

$$\mu \gg \left|\frac{\cot^3\psi}{2\psi}\right|, \quad (42)$$

and effectively attains the bound $i^{-1} = \cot^2\psi/\mu$ when

$$\mu \gg \left|\cot^2\psi\left(3 + \frac{7}{2}\cot^2\psi\right)\right|. \quad (43)$$

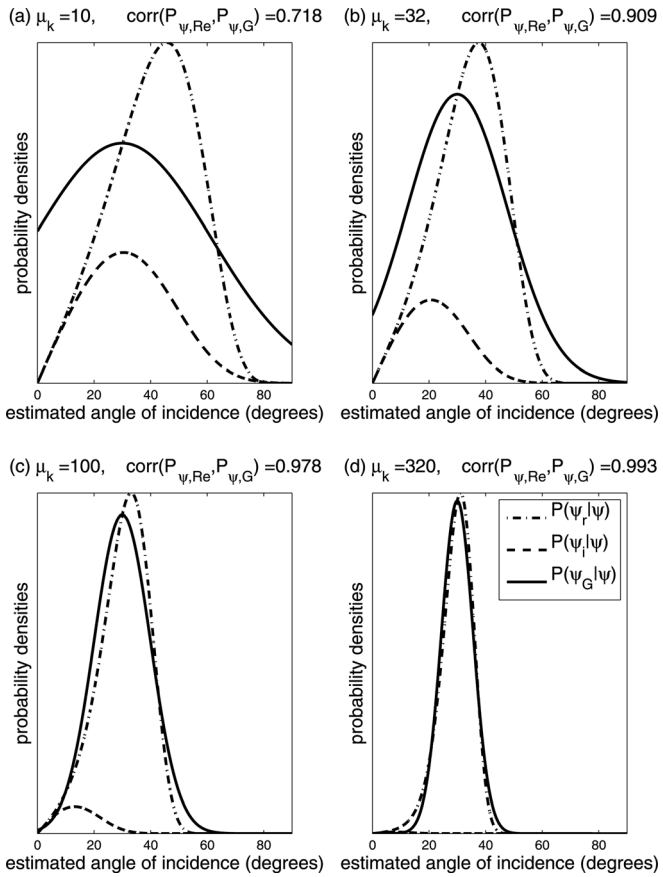

FIG. 2. Probability densities given real, imaginary, or Gaussian constraint on parameter estimate.

As the above expressions show, the sample size necessary for $\hat{\psi}$ to behave as a minimum variance, unbiased estimate varies nonlinearly from unity at shallow-grazing angles to infinity near normal incidence.

Figure 3 shows the sample sizes necessary for the MLE to become asymptotically unbiased [Eq. (42), dashed line], for the MLE variance to asymptotically attain the CRLB [Eq. (43), dashed-dotted line], and for the correlation between $P_{\hat{\psi},\mathrm{G}}$ and $P_{\hat{\psi},\mathrm{Re}}$, to be greater than 0.99 (solid line), as functions of the angle of incidence ψ. The curves have been truncated so that the minimum necessary sample size is 1. For most values of ψ, achieving a minimum variance estimate also ensures that an unbiased estimate is obtained that approximately obeys the Gaussian distribution of Eq. (41). For shallow-grazing incidence angles (ψ approaching 90 degrees), the sample size necessary for $P_{\hat{\psi},\mathrm{G}}$ to be a good approximation to $P_{\hat{\psi},\mathrm{Re}}$ becomes the limiting condition.

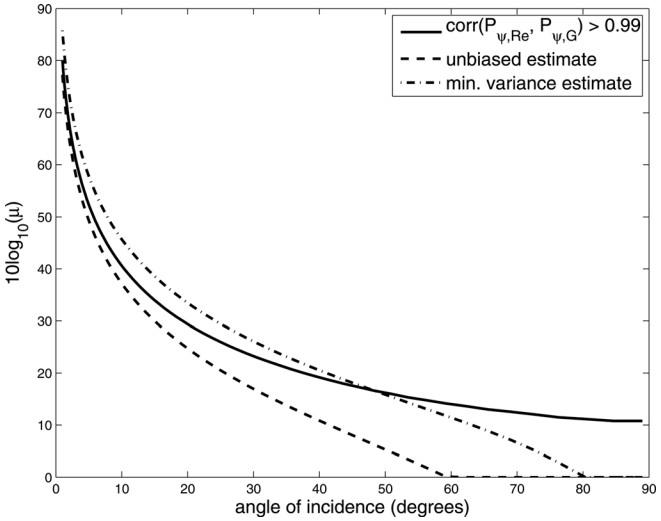

FIG. 3. Comparison of the necessary sample sizes to achieve (a) a correlation greater than 0.99 between and $P_{\hat{\psi},\mathrm{G}}(\hat{\psi};\psi)$, (b) an unbiased estimate, and (c) an estimate that attains the minimum possible variance.

C. 3D surface orientation and albedo

Two independent measurements of surface radiance with distinct illumination can lead to at most two unique solutions for the two components of Lambertian surface orientation.[13] This ambiguity in surface orientation can be easily resolved if one of the solutions places the surface out of the view of the observer. Otherwise, the ambiguity can be resolved if a third measurement is made under distinct illumination. These observations can be geometrically motivated by considering the intersection of the cones formed by appropriately rotating the Lambertian surface normals about the source direction for each measurement given the slope estimated from that measurement. Here, specific examples of resolution bounds on orientation estimation are presented, as well as expressions for the CRLBs for cone and polar angles, surface gradients and/or albedo given two or three measurements of surface radiance.

For surface gradient $\mathbf{a}^T=[p,\ q,\ \rho]$, or polar coordinate $\mathbf{a}^T=[\theta,\ \phi,\ \rho]$ parameterizations, the MSE bound on any unbiased estimate $\tilde{\mathbf{a}}$ is

$$\langle(\tilde{\mathbf{a}}-\mathbf{a})(\tilde{\mathbf{a}}-\mathbf{a})^T\rangle \geq \mathbf{i}_{\mathbf{a}}^{-1}=\frac{\partial \mathbf{a}}{\partial \mathbf{x}}\mathbf{i}_{\mathbf{x}}^{-1}\frac{\partial \mathbf{a}^T}{\partial \mathbf{x}}, \tag{44}$$

where $\mathbf{i}_{\mathbf{x}}$ is given in Eq. (25). The bound $\mathbf{i}_{\mathbf{a}}^{-1}$ becomes singular when all the $\mathbf{s}_k$ are coplanar but not tangent to the surface for non-zero $\boldsymbol{\sigma}_N$, or when the Jacobian $\frac{\partial \mathbf{a}}{\partial \mathbf{x}}$ is singular. When $\boldsymbol{\sigma}_N$ vanishes, $|\mathbf{i}_{\mathbf{x}}|^{1/2}\,|\mathbf{i}_{\boldsymbol{\sigma}}|^{-1/2}$ can be interpreted as the effective weighted volume of incident vectors $\mathbf{s}_k$. For example, when $\mathbf{R}$ is a 3D vector, the bound $\mathbf{i}_{\mathbf{x}}^{-1}$ is

$$[\mathbf{i}_{\mathbf{x}}^{-1}]_{ij}=\frac{\frac{\sigma_1^2}{\mu_1}[\mathbf{s}_2\times\mathbf{s}_3]_i[\mathbf{s}_2\times\mathbf{s}_3]_j+\frac{\sigma_2^2}{\mu_2}[\mathbf{s}_3\times\mathbf{s}_1]_i[\mathbf{s}_3\times\mathbf{s}_1]_j+\frac{\sigma_3^2}{\mu_3}[\mathbf{s}_1\times\mathbf{s}_2]_i[\mathbf{s}_1\times\mathbf{s}_2]_j}{(\mathbf{s}_1\cdot\mathbf{s}_2\times\mathbf{s}_3)^2}, \tag{45}$$

so that $|\mathbf{i}_{\mathbf{x}}|^{1/2}\ |\mathbf{i}_{\boldsymbol{\sigma}}|^{-1/2}$ simply is the volume $(\mathbf{s}_1 \cdot \mathbf{s}_2 \times \mathbf{s}_3)^2$ of the parallelepiped of incident vectors. Behavior of the Jacobian $\left|\frac{\partial \mathbf{a}}{\partial \mathbf{x}}\right|$ depends upon the final coordinates a, as can be seen from the respective forms $(p^2+q^2+1)^{3/2}/\rho^2$ and $1/(\rho^2 \sin^2\theta)$ for the surface gradient and polar systems.

Assume that the measurements R_k have the same number of coherence cells, $\mu_k = \mu$ for all k. The stereo case is considered where three measurements R_1, R_2 and R_3 are used to compute the two parameters a_1 and a_2. Let $a_1 = \alpha$ and $a_2 = \beta$ be the Lambertian surface orientations (azimuth and elevation angles, or surface gradients). The abbreviation $C_k = \sigma_k(\alpha,\beta) = \cos\psi[k]$ is used, where $\psi[k]$ denotes the angle of incidence for the k^{th} measurement. It is also convenient to define the vector $\boldsymbol{\Lambda}$ to have the elements $\Lambda_k = \ln C_k$, which contain the natural logarithms of the positive semi-definite measurement cosines. With this definition, the CRLB's for the general Lambertian surface orientations α and β follow from Eqns. (8) and (9), and are

$$E[(\hat{\alpha}-\alpha)^2] \geq \frac{1}{\mu} \frac{\left|\frac{\partial \boldsymbol{\Lambda}}{\partial \beta}\right|^2}{\left|\frac{\partial \boldsymbol{\Lambda}}{\partial \alpha} \times \frac{\partial \boldsymbol{\Lambda}}{\partial \beta}\right|^2}, \tag{46}$$

$$E[(\hat{\beta}-\beta)^2] \geq \frac{1}{\mu} \frac{\left|\frac{\partial \boldsymbol{\Lambda}}{\partial \alpha}\right|^2}{\left|\frac{\partial \boldsymbol{\Lambda}}{\partial \alpha} \times \frac{\partial \boldsymbol{\Lambda}}{\partial \beta}\right|^2}. \tag{47}$$

The bounds only depend upon the cosine between the source direction and Lambertian surface normal for each measurement, C_k, and the respective partial derivatives of these cosines with respect to the two orientation parameters to be estimated. It is relatively easy to determine conditions in which these expressions will attain limiting values due to the positive semi-definiteness of terms in the numerators and denominators. For example, the bounds are infinite when all three measurements are coplanar with the surface normal, such that $\mathbf{n} \cdot (\mathbf{s}[1] \times \mathbf{s}[2]) = \mathbf{n} \cdot (\mathbf{s}[2] \times \mathbf{s}[3]) = 0$. However, the bounds are not necessarily infinite for coplanar illumination directions that are not also coplanar with the surface normal, i.e. for $\mathbf{s}[1] \cdot (\mathbf{s}[2] \times \mathbf{s}[3]) = 0$, but $\mathbf{n} \cdot (\mathbf{s}[1] \times \mathbf{s}[2]) \neq 0$, or $\mathbf{n} \cdot (\mathbf{s}[2] \times \mathbf{s}[3]) \neq 0$. The bounds are zero when any of the two direction cosines C_1, C_2, C_3 are zero and the two respective illumination directions for these have differing polar angles.

It is also possible to estimate the albedo when three measurements with unique illumination directions are available. Let $a_3 = \rho$ be the surface albedo. It is useful to define the unit all-measurements-equal vector $\mathbf{E}$ by its components such that $E_k = 1$ for $k = 1, 2, 3$. With this definition, the CRLB's for estimation of α, β, ρ are given by

$$E[(\hat{\alpha}-\alpha)^2] \geq \frac{1}{\mu} \frac{\left|\frac{\partial \boldsymbol{\Lambda}}{\partial \beta} \times \mathbf{E}\right|^2}{\left[\left(\frac{\partial \boldsymbol{\Lambda}}{\partial \alpha} \times \frac{\partial \boldsymbol{\Lambda}}{\partial \beta}\right) \cdot \mathbf{E}\right]^2}, \tag{48}$$

$$E[(\hat{\beta}-\beta)^2] \geq \frac{1}{\mu} \frac{\left|\frac{\partial \boldsymbol{\Lambda}}{\partial \alpha} \times \mathbf{E}\right|^2}{\left[\left(\frac{\partial \boldsymbol{\Lambda}}{\partial \alpha} \times \frac{\partial \boldsymbol{\Lambda}}{\partial \beta}\right) \cdot \mathbf{E}\right]^2}, \tag{49}$$

$$E[(\hat{\rho}-\rho)^2] \geq \frac{\rho^2}{\mu} \frac{\left|\frac{\partial \boldsymbol{\Lambda}}{\partial \alpha} \times \frac{\partial \boldsymbol{\Lambda}}{\partial \beta}\right|^2}{\left[\left(\frac{\partial \boldsymbol{\Lambda}}{\partial \alpha} \times \frac{\partial \boldsymbol{\Lambda}}{\partial \beta}\right) \cdot \mathbf{E}\right]^2}, \tag{50}$$

It is noteworthy that the bound for ρ is a function of the surface orientation components α and β, as well as ρ. While the bounds for α and β given in Eqs. (48) and (49) are independent of the value of ρ, they are affected by uncertainty in the value of ρ, and Eqs. (46) and (47) are no longer applicable. These particular bounds for α and β are infinite when all three illumination directions are coplanar such that $\mathbf{s}[1] \cdot (\mathbf{s}[2] \times \mathbf{s}[3]) = 0$, even if the directions are not coplanar to the surface normal. Additionally, these bounds for α and β can be zero when any of the two direction cosines are zero.

Note that for the CRLB for ρ to be given by ρ^2/μ, and thereby be otherwise independent of Lambertian surface orientation, it is sufficient to have

$$\left(\frac{\partial \boldsymbol{\Lambda}}{\partial \alpha} \times \frac{\partial \boldsymbol{\Lambda}}{\partial \beta}\right) \cdot \mathbf{P} \left(\frac{\partial \boldsymbol{\Lambda}}{\partial \alpha} \times \frac{\partial \boldsymbol{\Lambda}}{\partial \beta}\right) = 0, \tag{51}$$

where the permutation matrix is defined as

$$\mathbf{P} = \begin{bmatrix} 0 & 1 & 0 \\ 0 & 0 & 1 \\ 1 & 0 & 0 \end{bmatrix}. \tag{52}$$

For example the CRLB for ρ is given by ρ^2/μ when any two of the measurement cosines C_1, C_2, C_3 are equal to zero.

Equations (48)–(50) are useful in providing a geometric interpretation of the CRLB for α, β and ρ given three measurements. For example, consider the conditions leading to the limiting values of zero and infinity for the bounds. Inspection of the positive semi-definite numerators and denominators of Eqs. (48)–(50) motivates consideration of the following two cases: (1) the partial derivative of the logarithmic measurement vector with respect to the orientation component α or β respectively is orthogonal to the all-measurements-equal vector; (2) the cross product of the partial derivatives of the logarithmic measurement vector with respect to the α and β orientations is orthogonal to the all-measurements-equal vector. When (1) is true but (2) is not, the respective bound on orientation component β or α is zero. When (1) is not true but (2) is true the bound on either orientation is infinite. As noted before, this occurs when the illumination directions for all measurements are coplanar with the surface normal. When both (1) and (2) are true, the bound on α or β depends only on the number of coherence cells.

Figure 4 shows the CRLB and the necessary sample sizes for the x-gradient p, in simultaneous estimation of p, q, and ρ with three incident illumination directions, s_1, s_2, and s_3. For illustrative purposes, only s_3 is allowed to vary. Optimal resolution [Fig. 4(b)], minimum necessary sample size

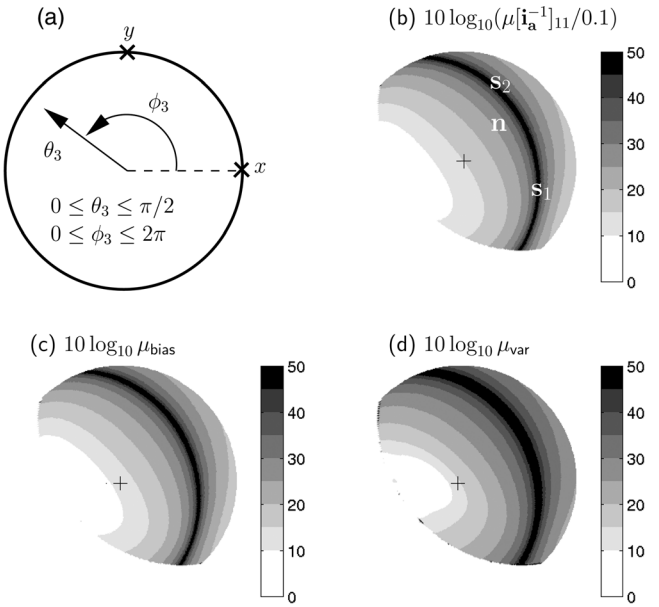

FIG. 4. A visualization for a corresponding to the surface gradient parameterization for a 3D measurement vector $\mathbf{R}$ with $\boldsymbol{\sigma}_N$ negligible and Lambertian surface defined by the polar coordinate parameterization ($\theta_n = \pi/4$, $\phi_n = \pi/4$, $\rho = 0.6$). Incident vectors $\mathbf{s}_1$ and $\mathbf{s}_2$ are fixed at [$\theta_1 = 0.3662\pi$ ($\approx 65.9°$), $\phi_1 = 1.8524\pi$ ($\approx 333°$)] and [$\theta_2 = 0.3662\pi$, $\phi_2 = 0.3524\pi$ ($\approx 63.4°$)], respectively, but $\mathbf{s}_3$ is allowed to vary as in (a) where the positive z-axis is central and points out of the page, the direction of the positive x-axis is the right-most point, and that of the positive y-axis is the top-most point, each marked by x and y, respectively. (b) The bound $[\mathbf{i}_\mathbf{a}^{-1}]_{11}$ on the x-gradient, $a_1 = p$, including full 3D coupling. Only values where $\mathbf{s}_3 \cdot \mathbf{n}$ is positive and the Lambertian surface is in view from the positive z-axis are shown. The incident vectors $\mathbf{s}_1$ and $\mathbf{s}_2$, and the surface normal $\mathbf{n}$ are marked by their respective symbols. The black cross marks the center ($\theta = 0$, $\phi = 0$). Optimal resolution (b), minimum necessary sample size for unbiased (c), and minimum variance (d) estimation, occurs when $\mathbf{s}_3$ is tangent to the Lambertian surface closest to the negative x-axis (extreme left), for the p-bound, so as to maximize the volume of incident vectors. Poorest resolution and largest sample sizes occur when the volume of incident vectors approaches zero, as realized along the dark arc in (b), (c), and (d). (c) The sample size necessary for the MLE $\hat{a}_1 = \hat{p}$ to be effectively unbiased, from Eq. (18). (d) The sample size necessary, from Eq. (19), for $\hat{p}$ to effectively attain the bound given in (b).

for unbiased [Fig. 4(c)] and minimum variance [Fig. 4(d)] estimation, occurs when $\mathbf{s}_3$ is tangent to the Lambertian surface closest to the negative x-axis for the p-bound, so as to maximize the volume of incident vectors. Poorest resolution and largest sample sizes, occur when the volume of incident vectors approaches zero, as realized along the dark arc in Figs. 4(b)–4(d). These computations exhibit the dramatic nonlinear variations in the sample sizes necessary to obtain accurate estimates of Lambertian surface orientation and albedo from multi-static acoustic, optical, radar or laser images corrupted by signal-dependent speckle noise. Similarly, the y-gradient is best resolved when $\mathbf{s}_3$ lies tangent to the surface and closest to the negative y-axis. Optimal albedo resolution is achieved as long as $\mathbf{s}_3$ lies tangent to the surface anywhere in the third θ, ϕ quadrant.

VI. CONCLUSIONS

A maximum likelihood method for estimating remote surface orientation from multi-static acoustic, optical, radar or laser images is derived. It is assumed that the images are corrupted by signal-dependent noise, known as speckle, arising from complex Gaussian field fluctuations, and that the surface properties are effectively Lambertian. Surface orientation estimates for a single sample are shown to have biases and errors that vary dramatically depending on illumination direction. This is due to the signal-dependent nature of speckle noise and the nonlinear relationship between surface orientation, illumination direction and fluctuating radiance. The minimum number of independent samples necessary for MLEs to be asymptotically unbiased and attain the lower bound on resolution of classical estimation theory are derived, as are practical design thresholds.

It is shown that the minimum error in estimating the angle of incidence of a Lambertian surface is at best proportional to the cotangent of this angle. The greatest accuracy occurs for estimates obtained from shallow illumination angles where Lambert's law shows its greatest sensitivity to surface illumination, while poorest resolution occurs near normal incidence where sensitivity is the least. For the general stereo case where at least three measurements are used to estimate 3D surface orientation and albedo, the minimum MSE is shown to be inversely proportional to the volume delimited by the unit normals of incident illumination. As a result, the number of samples or SNR necessary to accurately estimate surface orientation and albedo is shown to become arbitrarily large as the illumination directions approach the coplanar limit, while accurate stereo resolution of 3D surface orientation and albedo is shown to be possible even with a single sample given illumination directions of sufficient diversity and shallow angle incidence.

APPENDIX: EXPANSION OF BIAS AND VARIANCE IN INVERSE ORDERS OF SAMPLE SIZE OR SNR FOR GAMMA-DISTRIBUTED INTENSITY DATA

The explicit expressions presented in Ref. 26 for the asymptotic orders of the MLE bias and variance given general Gaussian random variables can also be used for random data that are not distributed in a Gaussian form provided that they can be expressed as the function of Gaussian random variables with a Jacobian of the transformation that is independent of the parameters to be estimated.[34,35] This result is then used to prove that the asymptotic orders of the MLE bias and variance are expressible in inverse orders of SNR when the measurement data follow the gamma distribution of Eq. (6).

Consider a single vector sample composed of $Y_1, \ldots, Y_b$ arbitrary random variables which can be expressed in terms of $u_1, \ldots, u_q$ Gaussian random variables ($q \ge b$). Assume that the Jacobian of the transformation is independent of the parameter vector a. The mapping is assumed to be one-to-one between $\mathbf{u} = [u_1, \ldots, u_q]^T$ and $\mathbf{Y} = [Y_1, \ldots, Y_b]^T$ (for $q = b$), or between $\mathbf{u}$ and $\mathbf{Y}' \equiv [\mathbf{Y}, \Omega]^T = [Y_1, \ldots, Y_b, \Omega_1, \ldots, \Omega_{q-b}]^T$ (for $q > b$), with $\Omega_1, \ldots, \Omega_{q-b}$ some arbitrary random variables that are not dependent on the parameter vector a. For the general case of $q > b$, the parameter-independent Jacobian of the transformation is $J' = \left|\frac{\partial \mathbf{u}}{\partial \mathbf{Y}'}\right|$. In this case, we have the following identity which holds for the expectation of any function of derivatives of the likelihood function with respect to the parameters,

$$\langle f\rangle_{\mathbf{Y}} = \int f\left(\frac{\partial \ln(p(\mathbf{Y};\mathbf{a}))}{\partial a},\ldots,\frac{\partial^b \ln(p(\mathbf{Y};\mathbf{a}))}{\partial a^b}\right)p(\mathbf{Y};\mathbf{a})\mathrm{d}\mathbf{Y}$$
$$= \int\int f\left(\frac{\partial \ln(p(\mathbf{Y};\mathbf{a})p(\Omega))}{\partial a},\ldots,\frac{\partial^b \ln(p(\mathbf{Y};\mathbf{a})p(\Omega))}{\partial a^b}\right) \times p(\mathbf{Y};\mathbf{a})p(\Omega)\mathrm{d}\mathbf{Y}\mathrm{d}\Omega \quad \text{(A1)}$$

where the last equality is introduced so as to make the transformation between $\mathbf{Y}'$ and $\mathbf{u}$, since $p(\mathbf{Y};\mathbf{a})p(\Omega) = p(\mathbf{u}(\mathbf{Y},\Omega;\mathbf{a}))J'$ and Ω is parameter independent. Equation (A1) can then be written as

$$\langle f\rangle_{\mathbf{Y}} = \int f\left(\frac{\partial \ln(p(\mathbf{u}(\mathbf{Y},\Omega);\mathbf{a})J')}{\partial a},\ldots,\frac{\partial^b \ln(p(\mathbf{u}(\mathbf{Y},\Omega);\mathbf{a})J')}{\partial a^b}\right) \times p(\mathbf{u}(\mathbf{Y},\Omega);\mathbf{a})J'\mathrm{d}\mathbf{Y}\mathrm{d}\Omega$$
$$= \int f\left(\frac{\partial \ln(p(\mathbf{u};\mathbf{a}))}{\partial a},\ldots,\frac{\partial^b \ln(p(\mathbf{u};\mathbf{a}))}{\partial a^b}\right)p(\mathbf{u};\mathbf{a})\mathrm{d}\mathbf{u} = \langle f\rangle_{\mathbf{u}}. \quad \text{(A2)}$$

The expected value of any function of derivatives of the likelihood function for $\mathbf{Y}$ with respect to the parameters $\mathbf{a}$ can then be written as the same function of derivatives of the likelihood function for $\mathbf{u}$. Since the asymptotic orders are the functions of expectations that have the same structure as Eq. (A1), the asymptotic orders of the MLE of a parameter a can be computed from measurements of the non-Gaussian quantity $\mathbf{Y}$.

For the problem of surface orientation considered here, the measurements $\mathbf{R}$, given parameter vector $\mathbf{a}$, are distributed according to the product of gamma distributions of Eq. (6). The parameter a can be estimated using the set of Gaussian random variables $x_{1,1},\ldots,x_{1,2\mu_1},x_{2,1},\ldots,x_{2,2\mu_2},\ldots,x_{M,1},\ldots,x_{M,2\mu_M}$, such that

$$P_{\mathbf{x}}(x_{1,1},\ldots,x_{M,2\mu_M};\mathbf{a}) = \prod_{k=1}^{M}\left(\prod_{i=1}^{2\mu_k}\frac{1}{\sqrt{\pi\sigma_k(\mathbf{a})}}\exp\left(-\frac{x_{k,i}^2}{\sigma_k(\mathbf{a})}\right)\right), \quad \text{(A3)}$$

where σ_k is the mean of R_k and also twice the variance of $x_{k,i}$ for $i=1,\ldots,2\mu_k$. Assuming that $\mu_k=\mu$ for all k, Eq. (A3) then becomes

$$P_{\mathbf{x}}(\mathbf{x}_1,\ldots,\mathbf{x}_{2\mu};\mathbf{a}) = \frac{1}{(2\pi)^{M\mu}|\mathbf{C}(\mathbf{a})|^{\mu}}\exp\left(-\frac{1}{2}\sum_{j=1}^{2\mu}\mathbf{x}_j^T\mathbf{C}(\mathbf{a})^{-1}\mathbf{x}_j\right) \quad \text{(A4)}$$

where $\mathbf{x}_j=[x_{1,j},\ldots,x_{M,j}]^T$ is the jth sample of the M-dimensional data vector for $j=1,\ldots,2\mu$, and the M-dimensional covariance matrix $\mathbf{C}(\mathbf{a})$ has elements $\mathbf{C}_{kl}=\delta_{kl}\sigma_k/2$. Using this notation, the M-dimensional measurement $\mathbf{R}$, with parameter-dependent mean $\boldsymbol{\sigma}(\mathbf{a})$, can be replaced by the measurement $\mathbf{x}$ obtained from $n=2\mu$ independent and identically distributed M-dimensional vectors, where the parameter dependence is instead on the covariance of the data, $\mathbf{C}(\mathbf{a})$.

The asymptotic orders of the MLE bias and variance for the rth component of the parameter vector a can then be determined using the existing expressions for the Gaussian case, Eq. (7) of Ref. 26 and Eq. (2.4) of Ref. 35 after substituting for $n'=2\mu$ and $\mathbf{C}_{kl}=\delta_{kl}\sigma_k/2$. Since μ is the SNR of the gamma-distributed $\mathbf{R}$ measurement, the MLE bias and variance given data that follow a gamma distribution can be written as asymptotic series in inverse orders of SNR,

$$\mathrm{bias}(\hat{a}_r,\boldsymbol{\mu},M=1) = \frac{b_1(\hat{a}_r;\mathbf{a},\mathbf{e},1)}{\mu}+\frac{b_2(\hat{a}_r;\mathbf{a},\mathbf{e},1)}{\mu^2}+O\left(\frac{1}{\mu^3}\right), \quad \text{(A5)}$$

$$\mathrm{var}(\hat{a}_r,\boldsymbol{\mu},M=1) = \frac{\mathrm{var}_1(\hat{a}_r;\mathbf{a},\mathbf{e},1)}{\mu}+\frac{\mathrm{var}_2(\hat{a}_r;\mathbf{a},\mathbf{e},1)}{\mu^2} + O\left(\frac{1}{\mu^3}\right), \quad \text{(A6)}$$

where the vector $\mathbf{e}$ with components $e_k=1$ signifies $\mu_k=\mu$ for all $k=1,2,\ldots,M$.

[1] J. C. Dainty, ed., *Laser Speckle and Related Phenomena*, 2nd ed. (Springer-Verlag, Berlin, 1984), pp. 1–7
[2] J. W. Goodman, "Statistical properties of laser speckle patterns," in *Laser Speckle and Related Phenomena*, 2nd ed., edited by J. C. Dainty (Springer-Verlag, Berlin, 1984), pp. 9–75.
[3] J. W. Goodman, *Statistical Optics* (Wiley, New York, 1985), pp. 41–43.
[4] G. Parry, "Speckle patterns in partially coherent light," in *Laser Speckle and Related Phenomena*, 2nd ed., edited by J. C. Dainty (Springer-Verlag, Berlin, 1984), pp. 77–122.
[5] N. C. Makris, "The effect of saturated transmission scintillation on ocean acoustic intensity measurements," J. Acoust. Soc. Am. **100**, 769–783 (1996).
[6] R. J. Urick, *Principles of Underwater Sound* (McGraw-Hill, New York, 1983), pp. 29–63.
[7] F. B. Jensen, W. A. Kuperman, M. B. Porter, and H. Schmidt, *Computational Ocean Acoustics* (AIP, New York, 1994), pp. 50–51.
[8] M. Born and E. Wolf, *Principles of Optics*, 7th ed. (Cambridge University Press, Cambridge, 1999), pp. 313–410.
[9] H. C. Van Du Hulst, *Light Scattering by Small Particles* (Dover, New York, 1981), pp. 110–113.
[10] T. L. Szabo, *Diagnostic Ultrasound Imaging: Inside Out* (Elsevier Science, Boston, 2004), pp. 213–240.
[11] S. A. Drury, *Image Interpretation in Geology*, 2nd ed. (Chapman and Hall, London, 1993), pp. 176–204.
[12] W. G. Egan, *Optical Remote Sensing Science and Technology* (Marcel Dekker, Inc., New York, 2004), pp. 1–27.
[13] B. K. P. Horn, *Robot Vision* (MIT Press, Cambridge, 1986), pp. 202–242.
[14] V. Murino and A. Trucco, "Three-dimensional image generation and processing in underwater acoustic vision," Proc. IEEE **88**(12), 1903–1948 (2000).
[15] J. L. Sutton, "Underwater acoustic imaging," Proc. IEEE **67**(4), 554–566 (1979).
[16] R.K. Hansen and P. A. Andersen, "3D Acoustic camera for underwater imaging," in *Acoustical Imaging*, edited by Y. Wei and B. Gu (Plenum, New York, 1993), Vol. 20, pp. 723–727.
[17] H. Singh, L. Whitcomb, D. Yoerger, and O. Pizarro, "Microbathymetric mapping from underwater vehicles in the deep ocean," Comput. Vis. Image Underst. **79**, 143–161 (2000).
[18] E. Chesters, "The use of a high-frequency pencil beam sonar to determine the position of tubular members of underwater structures," *in OCEANS '94. Oceans Engineering for Today's Technology and Tomorrow's Preservation*, (1994), Vol. 1, pp. I/ 199–I/204.
[19] E. Belcher, B. Matsuyama, and G. Trimble, "Object identification with acoustic lenses," *in Proceedings of Oceans 2001 Conference*, Honolulu, Hawaii (November 5–8, 2001), pp. 6–11.

[20]J. A. Panza, "Real-time three dimensional echocardiography: An overview," Int. J. Cardiovasc. Imaging **17**, 227–235 (2001).
[21]O. T. Von Ramm and S. W. Smith, "Real time volumetric ultrasound imaging system," J. Digit. Imaging 3(**4**), 261–266 (1990).
[22]C. A. Poynton, "'Gamma' and its disguises: The nonlinear mappings of intensity in perception, CRTs, film and video," SMPTE J. **102**, 1099–1108 (1993).
[23]L.R. Shenton and K. O. Bowman, *Maximum Likelihood Estimation in Small Samples* (Griffin, New York, 1977), p. 7.
[24]O.E. Barndorff-Nielsen and D. R. Cox, *Inference and Asymptotics* (Chapman and Hall, London, 1994), pp. 184–187.
[25]P. McCullagh, *Tensor Methods in Statistics (Monographs on Statistics and Applied Probability)* (Chapman and Hall, London, 1987), Chap. 7, p. 198.
[26]E. Naftali and N. C. Makris, "Necessary conditions for a maximum likelihood estimate to become asymptotically unbiased and attain the Cramer–Rao Lower Bound. Part I. General approach with an application to time-delay and Doppler shift estimation," J. Acoust. Soc. Am. **110**, 1917–1930 (2001).
[27]N. C. Makris, "Estimating surface orientation from sonar images," in *SACLANT Conference Proceedings Series CP-45* (1997), pp. 339–346.
[28]N. C. Makris, "A foundation for logarithmic measures of fluctuating intensity in pattern recognition," Opt. Lett. **20**, 2012–2014 (1995).
[29]C. R. Rao, *Linear Statistical Inference and Its Applications* (Wiley, New York, 1966), pp. 314–443.
[30]S. M. Kay, *Fundamentals of Statistical Signal Processing: Estimation Theory* (Prentice Hall, New Jersey, 1993), pp. 27–80.
[31]A. Thode, M. Zanolin, E. Naftali, I. Ingram, P. Ratilal, and N. C. Makris, "Necessary conditions for a maximum likelihood estimate to become asymptotically unbiased and attain the Cramer–Rao lower bound. Part II. Range and depth localization of a sound source in an ocean waveguide," J. Acoust. Soc. Am. **112**, 1890–1910 (2002).
[32]M. Zanolin, I. Ingram, A. Thode, and N. C. Makris, "Asymptotic accuracy of geoacoustic inversions," J. Acoust. Soc. Am. **116**, 2031–2042 (2004).
[33]R. A. Fisher, *Statistical Methods and Scientific Inference* (Hafner, New York, 1956), pp. 1–180.
[34]M. Zanolin, E. Naftali, and N. Makris, "Second-order bias of a multivariate Gaussian maximum likelihood estimate with chain-rule for higher moments," Technical Report No. 13-2003-37, Massachusetts Institute of Technology (2003).
[35]M. Zanolin, S. Vitale, and N. Makris, "Application of asymptotic expansions of maximum likelihood estimators errors to gravitational waves from binary mergers: The single interferometer case," Phys. Rev. D **81**(**12**), 124048.1–124048.16 (2010).